

Unveiling the origin of the gamma-ray emission in NGC 1068 with the Cherenkov Telescope Array

A. Lamastra,^{1,2} F. Tavecchio,³ P. Romano,³ M. Landoni,³ S. Vercellone³

¹ *INAF - Osservatorio Astronomico di Roma, via di Frascati 33, 00078 Monte Porzio Catone, Italy*

² *SSDC-ASI, via del Politecnico, 00133 Roma, Italy*

³ *INAF - Osservatorio Astronomico di Brera, via E. Bianchi 46, I-23807, Merate, Italy*

Abstract

Several observations are revealing the widespread occurrence of mildly relativistic wide-angle AGN winds strongly interacting with the gas of their host galaxy. Such winds are potential cosmic-ray accelerators, as supported by gamma-ray observations of the nearby Seyfert galaxy NGC 1068 with the *Fermi* gamma-ray space telescope. The non-thermal emission produced by relativistic particles accelerated by the AGN-driven wind observed in the circum-nuclear molecular disk of such galaxy is invoked to produce the gamma-ray spectrum. The AGN wind model predicts a hard spectrum that extend in the very high energy band which differs significantly from those corresponding to other models discussed in the literature, like starburst or AGN jet. We present dedicated simulations of observations through the Cherenkov Telescope Array (CTA), the next-generation ground based gamma-ray observatory, of the very high energy spectrum of the Seyfert galaxy NGC 1068 assuming the AGN wind and the AGN jet models. We demonstrate that, considering 50 hours of observations, CTA can be effectively used to constrain the two different emission models, providing important insight into the physics governing the acceleration of particles in non-relativistic AGN-driven outflows. This analysis strongly motivates observations of Seyfert and starburst galaxies with CTA in order to test source population models of the extragalactic gamma-ray and neutrino backgrounds.

Keywords:

galaxies: individual: NGC 1068, galaxies: Seyfert, gamma rays: galaxies

1. Introduction

Galactic winds driven by star formation and active galactic nuclei (AGN) play a key role in the evolution of galaxies. The galactic winds, powered by the momentum and energy injected by massive stars in the form of supernovae (SN), are believed to regulate the rate of star formation in low mass galaxies. In high-mass galaxies, galaxy formation models require AGN to inject energy and momentum into the surrounding gas in order to reproduce key observables of galaxy population, like the bright end of the galaxy luminosity function, and the tight scaling relations between supermassive black hole (SMBH) masses and galaxy bulge properties [e.g. 1, 2, 3, 4, 5, 6].

One way of coupling AGN energy and momentum with the gas in the host galaxy is through AGN-driven winds and jets. Jets are highly collimated relativistic outflows of particles which characterize radio loud AGN (which represent $\sim 10\%$ of the AGN population) and are especially prominent in blazars, in which one of the jets points close to our line of sight. The bulk of the AGN population does not show jet-like structure [see 7, for a review]. The active nucleus of these galaxies is observed to eject wider-angle wind of lower velocity. These winds are observed in different ionization states (ionized, neutral atomic, and molecular) and at different spatial scales (from nuclear to galactic scales) through spectroscopy in the X-ray, UV, and NIR bands, and interferometric observation in the sub-millimetre band [see 8, and references therein].

The most striking difference between jetted and non-jetted AGN is in the origin and nature of their electromagnetic emission. As inferred from blazars, relativistic jets emit a large fraction of their energy in the radio and gamma-ray bands through non-thermal processes. Conversely, the emission of non-jetted AGN is dominated by thermal emission in the UV-optical band produced by the accretion disk around SMBH.

Non-jetted AGN may emit also non-thermal radiation in the gamma-ray band, as indicated by the detection of nearby Seyfert galaxies NGC 1068, NGC 4945, and the Circinus galaxy with the *Fermi* gamma-ray space telescope [9, 10]. These observations has lead to consider non-jetted AGN as potential cosmic-ray (CR) accelerators, and it has also been suggested that the diffuse extragalactic gamma-ray background (EGB) measured by the Large Area Telescope (LAT, [11]) on board the *Fermi* telescope [12] could be reproduced by the cumulative gamma-ray emission from the whole AGN population ([13, 14], but see [15]).

In this paper, we assess the potentiality of the Cherenkov Telescope Array (CTA) to test CR acceleration models in non-blazar AGN, focusing on the test case of the prototypical Seyfert galaxy NGC 1068 that is a nearby ($D=14.4$ Mpc) Seyfert 2 galaxy in which AGN-driven molecular wind, and radio structures, similar to collimated outflows but weaker and slower than the jets observed in blazars, have been observed [16, 17, 18, 19, 20, 21, 22].

Moreover, it is the brightest of the star forming galaxies detected by *Fermi*-LAT [9]. The *Fermi* collaboration interpreted the gamma-ray detection in terms of CR associated to star-formation processes, adopting the paradigm that Galactic CR are relativistic particles accelerated in SN-driven winds, and that the gamma-ray emission is due to CR interaction with the galactic interstellar medium (ISM). However, some models assuming that the gamma-ray emission is entirely due to starburst activity underestimated the *Fermi*-LAT spectrum [23, 24]. This suggests that the active nucleus also contributes to the gamma-ray emission. In this framework, two different theoretical models have been proposed so far. A lepto-hadronic model in which the gamma-ray emission is produced by electrons and protons accelerated by the shocks produced by the AGN-driven molecular wind [25], and a leptonic model in which the gamma-ray emission is produced through inverse Compton (IC) scattering of low energy photons from the relativistic electrons accelerated in the radio jet [26].

The gamma-ray spectra predicted by the AGN wind and AGN jet models differ significantly at energies $E \gtrsim 100$ GeV, where imaging atmospheric Cherenkov telescopes (IACT) are more sensitive than *Fermi*-LAT. However, the sensitivity of current IACTs does not allow us to test the existence of the emission in the very high energy (VHE) band predicted by the AGN wind model. The construction of the CTA is expected to provide a broad (20 GeV-300 TeV) energy range, and an average differential sensitivity a factor 5-20 better with respect to the current IACTs. We performed dedicated simulations of observations through CTA of the gamma-ray spectrum of NGC 1068 predicted by the AGN wind and AGN jet models, in order to constrain the two competing scenarios.

The paper is organised as follows. In Section 2 we recall the basic points of the AGN wind and AGN jet models and illustrate the predicted spectral energy distributions (SED) used for the simulations; in Section 3 we describe the simulation set-up and present our results, while we give our discussion and conclusions in Section 4.

Table 1: AGN models and corresponding key quantities. W1÷W4= AGN wind models. Jet= AGN jet model.

| Model | $L_{\text{kin}}/L_{\text{AGN}}$ | n_{H} (cm^{-3}) | F_{cal} | B (G) | η_{p} | η_{e} | | | | |
|-------|---------------------------------|----------------------------------------|--------------------|---------------------|--------------------------------------------|----------------------|-------|-------|---------------------|-----------------------|
| W1 | 3×10^{-3} | 10^4 | 1 | 3×10^{-5} | 0.2 | 0.02 | | | | |
| W2 | 3×10^{-3} | 10^4 | 1 | 2×10^{-3} | 0.2 | 0.02 | | | | |
| W3 | 7×10^{-4} | 120 | 0.5 | 25×10^{-5} | 0.5 | 0.4 | | | | |
| W4 | 3×10^{-3} | 10^4 | 1 | 60×10^{-5} | 0.3 | 0.1 | | | | |
| Model | δ | B (G) | R (cm) | T (K) | L_{IR} (erg s^{-1}) | r (cm) | n_1 | n_2 | γ_{b} | γ_{max} |
| Jet | 1.2 | 10^{-4} | 2×10^{19} | 100 | 1.5×10^{42} | 2.2×10^{20} | 2.2 | 3.3 | 10^4 | 10^7 |

2. Theoretical models

In this section we briefly describe the AGN wind and AGN jet models, and we compare the predicted gamma-ray spectra with *Fermi*-LAT data.

2.1. AGN wind model

In [25] we presented a physical model for the gamma-ray emission produced by CR particles accelerated by the AGN-driven wind observed in the circumnuclear molecular disk of NGC 1068 [16, 17]. The gamma-ray emission has a hadronic component that originates from the decay of neutral pions produced in inelastic collisions between accelerated protons and ambient protons, and a leptonic component produced by IC scattering, and Bremsstrahlung radiation produced by the primary and secondary accelerated electrons. In this paper we have updated the AGN wind model by implementing the effects of the interaction of gamma-ray photons with the extragalactic background light (EBL), and the electromagnetic cascades initiated by high energy photons during their propagation in the intergalactic medium.

We assumed that protons and electrons are accelerated by the shocks produced by the AGN wind interaction with the surrounding ISM. The structure of the AGN wind-shock system is composed by a forward shock expanding into the ISM, and a reverse shock moving inwards, which are separated

by a contact discontinuity. Both the reverse and forward shock are likely sites of particle acceleration with an efficiency depending on radiative losses [27, 28, 29]. We assumed that diffusive shock acceleration (DSA) operates in AGN-driven shocks. Thus, the accelerated particle energy distribution can be expressed as a power-law with spectral index $p \simeq 2$ and an exponential high-energy cut-off [30, 31, 32, 33], and it is constrained by the wind dynamics and kinetic energy, and by the magnetic field in the shock region. The wind dynamics and kinetic energy are derived from observations in the millimetre band [16, 17]. The observationally derived quantities are the outflowing gas mass $M_{\text{out}} \simeq 1.8 \times 10^7 M_{\odot}$, the average radial extent of the outflow $R_{\text{out}} \simeq 100$ pc, and the projected radial outflow velocity $v_{\text{out}} \simeq (100-200)$ km s^{-1} , which give a wind kinetic luminosity equal to $L_{\text{kin}} = (0.5 - 1.5) \times 10^{42}$ erg s^{-1} . For the magnetic field B we assume the volume average ISM magnetic field strength $B = 6 \times (\Sigma_{\text{gas}}/0.0025 \text{ g cm}^{-2})^a \mu\text{G}$ where $a \simeq 0.4-1$ and $\Sigma_{\text{gas}} = (0.01-0.05) \text{ g cm}^{-2}$ is the disk gas surface density [34, 35, 36]. The latter corresponds to a gas number density $n_{\text{H}} = (115-460) \text{ cm}^{-3}$ assuming a cylindrical geometry with radius of 350 pc and vertical scale height $h \simeq 10$ pc [37]. The gas number density determines the efficiency of hadronic losses (F_{cal}) and free-free losses. The energy loss of relativistic electrons by IC scattering is determined by the AGN radiation energy density at the location of the shock $U_{\text{rad}} = L_{\text{AGN}}/4\pi c R_{\text{out}}^2$, we modelled the AGN SED with the synthetic spectrum computed by [38], and we normalized it to the bolometric luminosity of NGC 1068 $L_{\text{AGN}} = (0.4-2.1 \times 10^{45}) \text{ erg s}^{-1}$ [39, 40, 17, 41].

The particle energy-loss processes, and the size of the accelerator, determine the maximum energy of accelerated particles. As discussed in [25], the timescale on which particles are advected in the AGN wind ($\tau_{\text{adv}} = R_{\text{out}}/v_{\text{out}}$) is larger than the residence time of CR protons and electrons in the central nuclear disk of the galaxy, while diffusion losses are not taken into account (see e.g. [42] for a description of diffusion losses in the nuclei of starburst galaxies). The latter constitutes a source of uncertainty in the computation of the maximum proton energy that we estimate to be $E_{\text{max}} \simeq 10-100$ TeV.

Although NGC 1068 is a relatively nearby source, above few tens of TeV the effects of the interaction of gamma-ray photons with the IR emission spectrum of the EBL start to be important and determine the absorption of a substantial fraction of the flux, imprinting a well defined cut-off at the observed spectrum. The electron-positron pairs produced in this way, however, scatter off the photons of the CMB, triggering an electromagnetic cascade that reprocess the absorbed flux. Gamma-rays may also be absorbed by

radiation fields within the galaxy. The MID-IR and FAR-IR thermal dust emission from the ~ 1.5 -2 kpc starburst ring [43] that surrounds the acceleration region could provide the target photons for pair production with TeV gamma-rays. In this paper we take into account also these physical processes in deriving the gamma-ray spectrum predicted by the AGN wind model. For the EBL absorption we adopt the model by [44], and we find that it dominates over absorption of gamma-rays inside the galaxy. For the high energy electromagnetic cascades we use the convenient analytical treatment provided by [45]. The latter demonstrate that – in the case of nearby sources and monoenergetic injection at E_{inj} – a quite good approximation for the resulting cascade spectrum can be given in terms of a broken power law. Specifically, the spectrum can be written as:

$$F(E) = \begin{cases} k \left(\frac{E}{E_X}\right)^{-0.5} & , \quad E < E_X , \\ k \left(\frac{E}{E_X}\right)^{-0.98} & , \quad E_X < E < E_{\text{inj}} \end{cases} \quad (1)$$

where

$$E_X = \frac{1}{3} \left(\frac{E_{\text{inj}}}{m_e c^2}\right)^2 \epsilon_{\text{CMB}}, \quad (2)$$

and $\epsilon_{\text{CMB}} = 6.3 \times 10^{-4}$ eV is the photon energy of background radiation. The normalization constant k can be derived by integrating the flux absorbed through the interaction with the EBL. This description is strictly valid for monoenergetic gamma-rays but for our purposes we can use it even if we have a relatively broad absorbed spectrum. In that case we can expect that the main effect is to have, instead of the pronounced breaks given by Eq. 1, smoother changes of the slopes. In our calculations we assume $E_{\text{inj}} = 100$ TeV.

In Figure 1 we compare the resulting gamma-ray spectra with those obtained by [25] for different combinations of model parameters (see Table 1). In these models the galaxy and AGN properties were varied within their observational ranges, and both standard electron (η_e) and proton (η_p) acceleration efficiencies (W1 and W2 models), and acceleration efficiencies larger than those predicted by the standard acceleration theory were adopted (W3 and W4 models). As expected, the spectra predicted in this work differ significantly from those obtained by [25] only above $E=10$ TeV. As input of the simulations we consider only the revised spectral models derived in this work.

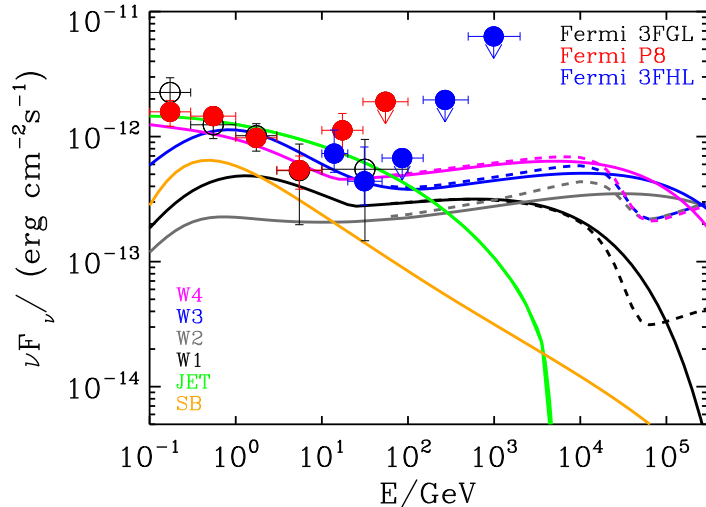


Figure 1: Gamma-ray spectrum of NGC 1068. The data points are from [46] (3FGL), from [25] (P8), and from [47] (3FHL). The green solid line shows the AGN jet model prediction. The black, grey, blue, and magenta solid lines show the AGN wind model predictions derived by [25], while dashed lines show the AGN wind model prediction taking into account the EBL absorption and electromagnetic cascades. For comparison, the gamma-ray spectrum predicted by the starburst model [24] is shown with the orange solid line.

The W1 and W2 models underestimate the *Fermi*-LAT spectrum, however, even if the gamma-ray emission predicted by these models is not the dominant contribution in the *Fermi*-LAT band, it could be relevant in the CTA band, so we performed the simulations also for these models.

2.2. AGN jet model

An alternative to the hadronic scenario discussed above is a leptonic model based on the assumption that the observed gamma-ray emission is produced by relativistic electrons flowing into a jet. In fact, as proposed by [26], the large gamma-ray emission from NGC 1068 could originate from the IC emission of relativistic electrons accelerated within a mildly relativistic collimated outflow expelled from the nucleus. In this scenario electrons could scatter both the synchrotron radiation (SSC) and the IR radiation of the surrounding environment. For reasonable values of the model parameters the latter component is expected to dominate.

We reproduce the inverse Compton spectrum of [26] using the code fully described in [48]. Briefly, the emission is produced in a spherical region with radius $R = 2 \times 10^{19}$ cm carrying a tangled magnetic field with intensity $B = 0.1$ mG in relativistic motion, parametrized by the relativistic Doppler factor $\delta = 1.2$. Electrons – following a smoothed broken power law energy distribution with normalization $K = 12.5 \text{ cm}^{-3}$ and slopes $n_1 = 2.2$ and $n_2 = 3.3$ below and above a Lorentz factor $\gamma_b = 10^4$ and with maximum Lorentz factor $\gamma_{max}=10^7$ – emit synchrotron and IC radiation. Following [26] we assume that the IR external field is modeled as a black body at a temperature $T = 100$ K, a luminosity $L_{\text{IR}} = 1.5 \times 10^{42} \text{ erg s}^{-1}$ occupying a spherical volume of radius $r = 2.2 \times 10^{20}$ cm.

The AGN jet model parameters are summarized in Table 1, and the IC spectrum is reported in Fig. 1 (green solid line). The *Fermi*-LAT data set the (relatively soft) slope of the high-energy electrons. The maximum energy of the electrons is a free parameter. We assume a maximum Lorentz factor $\gamma_{max} = 10^7$, i.e. a maximum energy of about 10 TeV. However, for the large value assumed for the maximum Lorentz factor of the emitting electrons, the resulting IC spectrum is only moderately dependent on the precise value of γ_{max} , since the cut-off visible in Fig. 1 is shaped by the transition to the Klein-Nishina regime. Indeed, for larger value of γ_{max} the high-energy cut-off does not move to much larger energies.

3. Simulations

3.1. Set-up

We performed our simulations using the analysis package `ctools` v.1.4.2 [49]¹, following the method described in [50], and the public CTA instrument response files (IRF, v. prod3b-v1). The source is located at RA(J2000) = 40.669583 deg, Dec(J2000) = -0.013333 deg, so it is visible from both CTA sites, at zenith angles of $\sim 29^\circ$ from the North and $\sim 24^\circ$ from the South. We therefore chose the `North_z20_average_50h` and `South_z20_average_50h` IRFs. The CTA Southern site baseline array is located at the European Southern Observatory in the Atacama Desert (Chile), and is planned to be composed of 4 large-sized telescopes (LSTs), 25 medium-sized telescopes (MSTs), and 70 small-sized telescopes (SSTs), while in the Northern site,

¹<http://cta.irap.omp.eu/ctools/>.

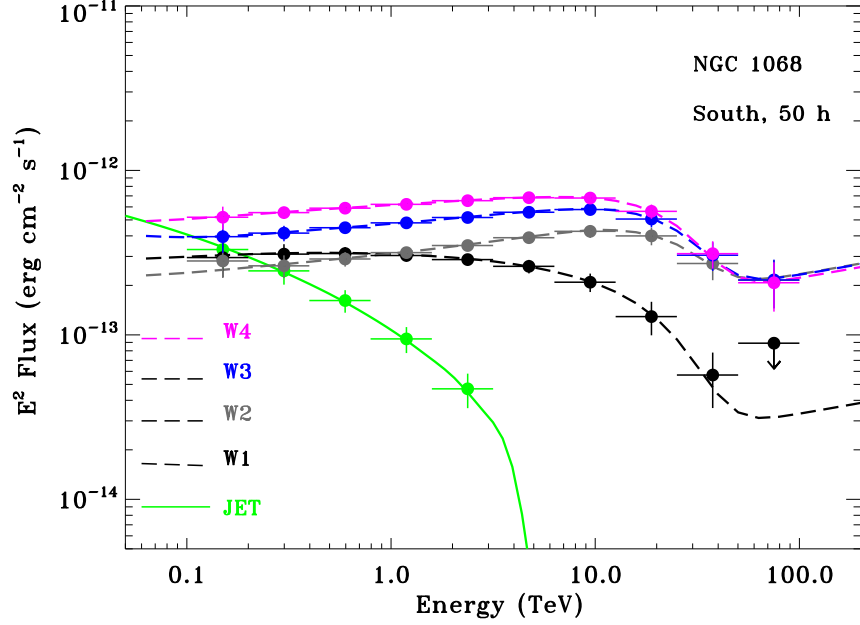


Figure 2: Simulated spectra of NGC 1068, color coded as in Fig. 1. See text for details.

Table 2: Array of `ctools` simulations. W1÷W4= AGN wind models. Jet= AGN jet model.

| Model | Site | zAngle (deg) | IRF | Expo (h) | Bins | Energy (TeV) | Number |
|-------|------|-----------------|-----------------------|-------------|------|-----------------|--------|
| W1 | S | 20 | South_z20_average_50h | 50h | 10 | 0.1–100 | 1000 |
| W2 | S | 20 | South_z20_average_50h | 50h | 10 | 0.1–100 | 1000 |
| W3 | S | 20 | South_z20_average_50h | 50h | 10 | 0.1–100 | 1000 |
| W4 | S | 20 | South_z20_average_50h | 50h | 10 | 0.1–100 | 1000 |
| Jet | N | 20 | North_z20_average_50h | 50h | 5 | 0.1–3.2 | 1000 |
| Jet | S | 20 | South_z20_average_50h | 50h | 5 | 0.1–3.2 | 1000 |

located at the Observatorio del Roque de los Muchachos on the island of La Palma (Spain), 4 LSTs and 15 MSTs are planned to be installed.

The SSTs contribution to the CTA sensitivity becomes dominant over the MSTs above a few TeV. Since wind models predict emission up to energies of about 100 TeV, the northern site results less favourable when considering wind models with respect to the jet one, which, on the contrary, shows a possible fall-off below 10 TeV. For this reason we discuss our simulations performed for the southern site and for both CTA sites when considering wind and jet models, respectively. A summary of the inputs to our simulations is reported in Table 2.

In the model definition XML file, the spectral model component was introduced as a “FileFunction” type, with the differential flux values described according to

$$M_{\text{spectral}}(E) = N_0 \frac{dN}{dE}, \quad (3)$$

where N_0 is the normalisation. We only considered the instrumental background included in the IRFs files (`CTAIrfBackground`) and no further contaminating astrophysical sources in the 5 deg field of view (FOV) we adopted for event extraction.

We considered a set of 10 energy bins covering an energy range reported in Table 2 (Col. 7). For the last model, we only considered 5 bins. In each bin, `ctobssim` was used to create event lists based on our input models. Then, the task `ctlike` was used to fit each spectral bin with a power-law model

$$M_{\text{spectral}}(E) = k_0 \left(\frac{E}{E_0} \right)^\Gamma, \quad (4)$$

where k_0 is the normalisation (or `Prefactor`, in units of $\text{ph cm}^{-2} \text{s}^{-1} \text{MeV}^{-1}$), E_0 is the pivot energy (`PivotEnergy` in MeV), and Γ is the power-law photon index (`Index`). In the fits `PivotEnergy` was fixed at 10^6 MeV, while `Prefactor` and `Index` were left to vary. We thus obtained the spectral parameters and fluxes of our gamma ray source in each bin by using maximum likelihood model fitting. Statistical uncertainties of the parameters were also calculated, as well as the test statistic (TS) value [51, 52]. For each spectral model $N = 1000$ sets of statistically independent realisations were created by adopting a different seed for the randomization in order to reduce the impact of variations between individual realisations [see, e.g. 49]. We thus obtained a set of 1000 values of each spectral parameter (and TS) from which 1000

values of fluxes were calculated in each energy bin. For each energy bin, we adopted as flux and error the mean and the square root of the standard deviation obtained from the distribution of fluxes².

3.2. Results

Figure 2 shows the spectra obtained with the simulations. For each model we report the input spectrum and the reconstructed spectrum in bins of energy. In the case of the AGN jet model, the simulation shows that the spectrum can be detected only up to energies $E \simeq 3$ TeV. In fact, the high-energy cut-off in the spectrum caused by the maximum energy of accelerated leptons implies no signal at the highest energy. On the other hand, the hadronic component predicted by the AGN wind model produces a spectrum that extends up to $E \simeq 100$ TeV. The simulations show that the high energy emission can be tracked in the whole energy range up to $E \simeq 100$ TeV for the W2, W3, and W4 models, and up to $E \simeq 50$ TeV in the case of W1 model.

These simulations imply that, considering 50 hours of observations, CTA can be effectively used to constrain the two different emission models. In fact, a detection at $E \gtrsim 10$ TeV will provide a smoking gun for the existence of a hadronic component in the gamma-ray spectrum of NGC 1068. To give an idea of the significance of the detection, we report the average and the standard deviation of the TS value obtained from the $N=1000$ sets of statistically independent realisations, in the last bin where we obtained a significant detection: 12.6-25.1 TeV in the case of W1 model: $\langle TS \rangle_{W1} = 111.3 \pm 33.1$, and for the energy bin 25.1-50.1 TeV for the other wind models: $\langle TS \rangle_{W2} = 194.2 \pm 48.4$, $\langle TS \rangle_{W3} = 225.4 \pm 52.5$, $\langle TS \rangle_{W4} = 233.1 \pm 52.0$. The only marginal critical point is the last detected energy bin for which we show in Figure 3 the whole TS distributions. Figure 3 shows that for the majority of the realizations the TS value is greater than 25 implying a significant detection also at the highest energies.

Moreover, the expectedly unprecedented sensitivity of CTA will allow us to reach a photon statistics able to determine fundamental features of the gamma-ray spectrum, like the position of the high energy cut-off. Therefore, as it will be discussed in the next Section, CTA observations of NGC 1068 will provide valuable constraints on the physics of the shock waves produced by AGN-driven winds.

²Mean flux $\overline{F_{\text{sim}}} = \frac{1}{N} \sum_{k=1}^N F_{\text{sim}}(k)$, standard deviation $s_{\text{sim}}^2 = \frac{1}{N-1} \sum_{k=1}^N (F_{\text{sim}}(k) - \overline{F_{\text{sim}}})^2$.

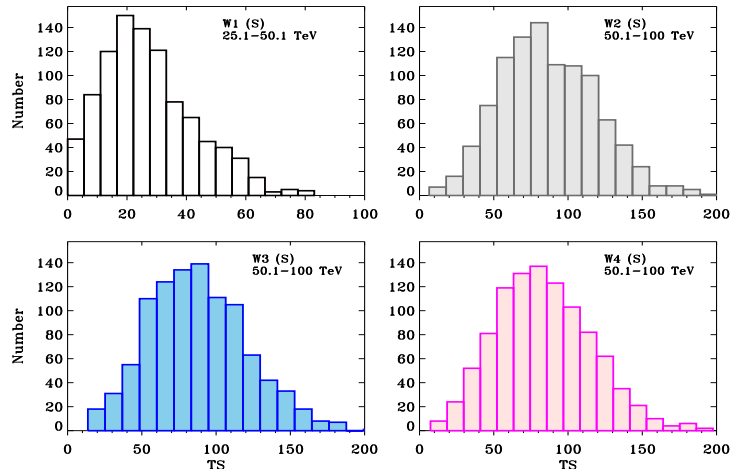


Figure 3: TS value distribution of the 1000 realizations in the last bin where we obtained a significant detection: 25.1-50.1 TeV (W1), and 50.1-100 TeV (W2,W3,W4) for the AGN wind model.

4. Discussion

The simulations presented in this work indicate that with 50 hours of observation with CTA we will be able to constrain emission models in NGC 1068. In fact, in case of signal detection at energies $E \gtrsim 10$ TeV, a pure jet model will be firmly excluded. The simulations indicate that the sensitivity and energy coverage of CTA allows us to measure with good accuracy the normalization and the position of the high energy cut-off of the gamma-ray spectrum.

Extending the spectrum to TeV energies is crucial to better constrain the non-thermal high energy luminosity of the source, and to compare it with the AGN and galaxy bolometric luminosity. From this comparison we might be able to determine if the hadronic gamma-ray emission is dominated by star formation or nuclear activity. At the highest energies, the AGN wind model predicts a spectral hardening above ~ 50 TeV. With a longer exposure CTA might reveal this spectral feature providing stringent constraints on hadronic models.

The detection of a high energy cut-off provide information on the max-

imum energy of accelerated particles which depends on shock parameters. In the case of protons, the maximum energy depends on the shock velocity, size of the accelerator, and on the magnetic field strength in the shock region. It has been suggested that protons accelerated by AGN-driven winds reach energies up to $E_{\max} \simeq 10\text{-}100$ PeV [53, 54, 25, 14, 15], the observational evidence of this hypothesis could have important implications for models of PeV neutrinos sources detected by IceCube [55, 56].

The comparison between the total non-thermal luminosity of NGC 1068 with the AGN wind kinetic luminosity inferred from millimetre spectroscopy (see Section 2) could constrain particle acceleration efficiencies (η_p and η_e) and the calorimetric efficiency (F_{cal}) in AGN-driven winds. The W1 and W2 models proposed by [25] are obtained by viewing AGN-driven wind as SN-driven wind analogue, thus values of η_p and η_e determined from SN observation in the radio and gamma-ray band are adopted [57, 58, 59, 35, and references therein]. However, the parameters that determine the physics of shock waves in the region near the AGN, like the pre-shock magnetic field and ISM density, could be not the same as those in non-active galaxies resulting in larger acceleration efficiencies than those predicted by the standard acceleration theory (W3 and W4 models). The determination of the normalization of the spectrum at TeV energies puts strong constraints on the values of η_p and η_e in AGN-driven winds.

As for the calorimetric fraction, to date there is no measurement of F_{cal} in AGN-driven winds. Assuming the standard SN paradigm for the gamma-ray emission in NGC 1068, values of $F_{\text{cal}} \gtrsim 1$ have been obtained by various authors [9, 60, 61]. This argues for a significant contribution of the active nucleus to the gamma-ray emission. Also in the other two Seyfert galaxies detected in the gamma-ray band, high efficiencies of gamma-ray production are predicted by the starburst scenario: $F_{\text{cal}} \simeq 1$ for NGC 4945, and $F_{\text{cal}} \gg 1$ for Circinus [26, 10, 60, 61]. Similarly to NGC 1068, AGN-driven molecular winds and weak radio jets have been observed in NGC 4945 and Circinus [62, 63, 64, 65]. These galaxies also show similarity of their Eddington-scaled X-ray and gamma-ray luminosity with $L_{0.1\text{-}100\text{GeV}}/L_{\text{Edd}} \simeq 10^{-4}$ and $L_{2\text{-}10\text{keV}}/L_{\text{Edd}} \simeq 10^{-2}$ in all three sources [66, 60], corroborating a correlation between the AGN activity and gamma-ray emission.

The gamma-ray spectra of these Seyfert galaxies, as well as of starburst galaxies, detected by *Fermi*-LAT and current IACTs, are shown in Figure 4. The starburst galaxies M82 and NGC 253 have already been detected in the VHE band by VERITAS, and H.E.S.S., respectively [67, 68, 69]. The

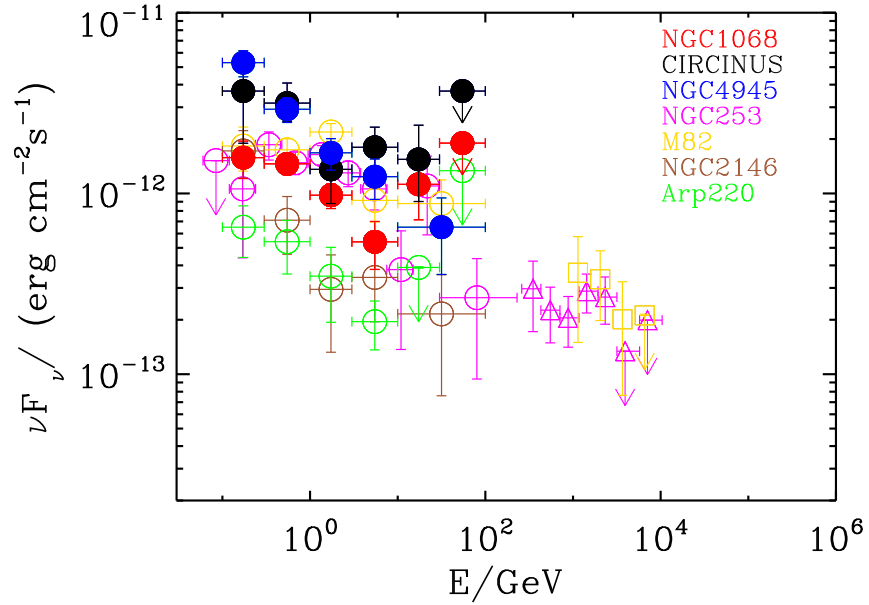


Figure 4: Gamma-ray spectra of Seyfert galaxies (filled symbols) and starburst galaxies (open symbols) detected by *Fermi*-LAT and IACTs. The data points are from [9, 46, 25, 47, 60, 10, 67, 72, 73, 69].

nearby ultra luminous infrared galaxy Arp 220 was observed by MAGIC and VERITAS but no significant excess over the background was found [70, 71].

The all-sky coverage and good sensitivity of the CTA full array will provide an unprecedented opportunity to improve our understanding of the gamma-ray emission in Seyfert and starburst galaxies that is crucial to test models of gamma-ray and neutrino sources that contribute to the extragalactic backgrounds observed by *Fermi*-LAT and IceCube [12, 55, 56].

Acknowledgements

The authors acknowledge contribution from the grant INAF CTA–SKA, “Probing particle acceleration and γ -ray propagation with CTA and its precursors” (PI F. Tavecchio).

AL acknowledges contribution from the grant INAF CTA–SKA “ASTRI/CTA Data Challenge” (PI P. Caraveo).

This research has made use of the NASA/IPAC Extragalactic Database (NED) which is operated by the Jet Propulsion Laboratory, California Institute of Technology, under contract with the National Aeronautics and Space Administration.

This research made use of `ctools`, a community-developed analysis package for Imaging Air Cherenkov Telescope data. `ctools` is based on `GammaLib`, a community-developed toolbox for the high-level analysis of astronomical gamma-ray data.

This research has made use of the CTA instrument response functions provided by the CTA Consortium and Observatory, see <https://www.cta-observatory.org/science/cta-p> (version prod3b-v1) for more details.

We gratefully acknowledge financial support from the agencies and organizations listed here: http://www.cta-observatory.org/consortium_acknowledgments.

This paper went through internal review by the CTA Consortium.

We thank L. Stawarz and J. P. Lenain as internal CTA reviewers.

References

- [1] A. R. King, K. A. Pounds, Black hole winds, *MNRAS* 345 (2003) 657–659 (Oct. 2003). [arXiv:astro-ph/0305541](https://arxiv.org/abs/astro-ph/0305541), [doi:10.1046/j.1365-8711.2003.06980.x](https://doi.org/10.1046/j.1365-8711.2003.06980.x).
- [2] T. Di Matteo, V. Springel, L. Hernquist, Energy input from quasars regulates the growth and activity of black holes and their host galaxies, *Nature* 433 (2005) 604–607 (Feb. 2005). [arXiv:arXiv:astro-ph/0502199](https://arxiv.org/abs/astro-ph/0502199), [doi:10.1038/nature03335](https://doi.org/10.1038/nature03335).
- [3] D. J. Croton, V. Springel, S. D. M. White, G. De Lucia, C. S. Frenk, L. Gao, A. Jenkins, G. Kauffmann, J. F. Navarro, N. Yoshida, The many lives of active galactic nuclei: cooling flows, black holes and the luminosities and colours of galaxies, *MNRAS*

- 365 (2006) 11–28 (Jan. 2006). [arXiv:arXiv:astro-ph/0508046](#), [doi:10.1111/j.1365-2966.2005.09675.x](#).
- [4] N. Menci, A. Fontana, E. Giallongo, A. Grazian, S. Salimbeni, The Abundance of Distant and Extremely Red Galaxies: The Role of AGN Feedback in Hierarchical Models, *ApJ* 647 (2006) 753–762 (Aug. 2006). [arXiv:arXiv:astro-ph/0605123](#), [doi:10.1086/505528](#).
- [5] R. S. Somerville, P. F. Hopkins, T. J. Cox, B. E. Robertson, L. Hernquist, A semi-analytic model for the co-evolution of galaxies, black holes and active galactic nuclei, *MNRAS* 391 (2008) 481–506 (Dec. 2008). [arXiv:0808.1227](#), [doi:10.1111/j.1365-2966.2008.13805.x](#).
- [6] A. Lamastra, N. Menci, R. Maiolino, F. Fiore, A. Merloni, The building up of the black hole-stellar mass relation, *MNRAS* 405 (2010) 29–40 (Jun. 2010). [arXiv:1001.5407](#), [doi:10.1111/j.1365-2966.2010.16439.x](#).
- [7] P. Padovani, D. M. Alexander, R. J. Assef, B. De Marco, P. Giommi, R. C. Hickox, G. T. Richards, V. Smolčić, E. Hatziminaoglou, V. Mainieri, M. Salvato, Active galactic nuclei: what’s in a name?, *A&AR* 25 (2017) 2 (Aug. 2017). [arXiv:1707.07134](#), [doi:10.1007/s00159-017-0102-9](#).
- [8] F. Fiore, C. Feruglio, F. Shankar, M. Bischetti, A. Bongiorno, M. Brusa, S. Carniani, C. Cicone, F. Duras, A. Lamastra, V. Mainieri, A. Marconi, N. Menci, R. Maiolino, E. Piconcelli, G. Vietri, L. Zappacosta, AGN wind scaling relations and the co-evolution of black holes and galaxies, *ArXiv e-prints* (Feb. 2017). [arXiv:1702.04507](#).
- [9] M. Ackermann, M. Ajello, A. Allafort, L. Baldini, J. Ballet, D. Bastieri, K. Bechtol, R. Bellazzini, B. Berenji, E. D. Bloom, E. Bonamente, A. W. Borgland, A. Bouvier, J. Bregeon, M. Brigida, P. Bruel, R. Buehler, S. Buson, G. A. Caliandro, R. A. Cameron, P. A. Caraveo, J. M. Casandjian, C. Cecchi, E. Charles, A. Chekhtman, C. C. Cheung, J. Chiang, A. N. Cillis, S. Ciprini, R. Claus, J. Cohen-Tanugi, J. Conrad, S. Cutini, F. de Palma, C. D. Dermer, S. W. Digel, E. d. C. e. Silva, P. S. Drell, A. Drlica-Wagner, C. Favuzzi, S. J. Fegan, P. Fortin, Y. Fukazawa, S. Funk, P. Fusco, F. Gargano, D. Gasparrini, S. Germani, N. Giglietto, F. Giordano, T. Glanzman, G. Godfrey, I. A. Grenier, S. Guiriec,

- M. Gustafsson, D. Hadasch, M. Hayashida, E. Hays, R. E. Hughes, G. Jóhannesson, A. S. Johnson, T. Kamae, H. Katagiri, J. Kataoka, J. Knödlseider, M. Kuss, J. Lande, F. Longo, F. Loparco, B. Lott, M. N. Lovellette, P. Lubrano, G. M. Madejski, P. Martin, M. N. Mazziotta, J. E. McEnery, P. F. Michelson, T. Mizuno, C. Monte, M. E. Monzani, A. Morselli, I. V. Moskalenko, S. Murgia, S. Nishino, J. P. Norris, E. Nuss, M. Ohno, T. Ohsugi, A. Okumura, N. Omodei, E. Orlando, M. Ozaki, D. Parent, M. Persic, M. Pesce-Rollins, V. Petrosian, M. Pierbattista, F. Piron, G. Pivato, T. A. Porter, S. Rainò, R. Rando, M. Razzano, A. Reimer, O. Reimer, S. Ritz, M. Roth, C. Sbarra, C. Sgrò, E. J. Siskind, G. Spandre, P. Spinelli, L. Stawarz, A. W. Strong, H. Takahashi, T. Tanaka, J. B. Thayer, L. Tibaldo, M. Tinivella, D. F. Torres, G. Tosti, E. Troja, Y. Uchiyama, J. Vandenbroucke, G. Vianello, V. Vitale, A. P. Waite, M. Wood, Z. Yang, GeV Observations of Star-forming Galaxies with the Fermi Large Area Telescope, *ApJ* 755 (2012) 164 (Aug. 2012). [arXiv:1206.1346](#), [doi:10.1088/0004-637X/755/2/164](#).
- [10] M. Hayashida, L. Stawarz, C. C. Cheung, K. Bechtol, G. M. Madejski, M. Ajello, F. Massaro, I. V. Moskalenko, A. Strong, L. Tibaldo, Discovery of GeV Emission from the Circinus Galaxy with the Fermi Large Area Telescope, *ApJ* 779 (2013) 131 (Dec. 2013). [arXiv:1310.1913](#), [doi:10.1088/0004-637X/779/2/131](#).
- [11] W. B. Atwood, A. A. Abdo, M. Ackermann, W. Althouse, B. Anderson, M. Axelsson, L. Baldini, J. Ballet, D. L. Band, G. Barbiellini, et al., The Large Area Telescope on the Fermi Gamma-Ray Space Telescope Mission, *ApJ* 697 (2009) 1071–1102 (Jun. 2009). [arXiv:0902.1089](#), [doi:10.1088/0004-637X/697/2/1071](#).
- [12] M. Ackermann, M. Ajello, A. Albert, W. B. Atwood, L. Baldini, J. Ballet, G. Barbiellini, D. Bastieri, K. Bechtol, R. Bellazzini, E. Bissaldi, R. D. Blandford, E. D. Bloom, E. Bottacini, T. J. Brandt, J. Bregeon, P. Bruel, R. Buehler, S. Buson, G. A. Caliandro, R. A. Cameron, M. Caragiulo, P. A. Caraveo, E. Cavazzuti, C. Cecchi, E. Charles, A. Chekhtman, J. Chiang, G. Chiaro, S. Ciprini, R. Claus, J. Cohen-Tanugi, J. Conrad, A. Cuoco, S. Cutini, F. D’Ammando, A. de Angelis, F. de Palma, C. D. Dermer, S. W. Digel, E. d. C. e. Silva, P. S. Drell, C. Favuzzi, E. C. Ferrara, W. B. Focke, A. Franckowiak,

- Y. Fukazawa, S. Funk, P. Fusco, F. Gargano, D. Gasparri, S. Germani, N. Giglietto, P. Giommi, F. Giordano, M. Giroletti, G. Godfrey, G. A. Gomez-Vargas, I. A. Grenier, S. Guiriec, M. Gustafsson, D. Hadasch, K. Hayashi, E. Hays, J. W. Hewitt, P. Ippoliti, T. Jogler, G. Jóhannesson, A. S. Johnson, W. N. Johnson, T. Kamae, J. Kataoka, J. Knödseder, M. Kuss, S. Larsson, L. Latronico, J. Li, L. Li, F. Longo, F. Loparco, B. Lott, M. N. Lovellette, P. Lubrano, G. M. Madejski, A. Manfreda, F. Massaro, M. Mayer, M. N. Mazziotta, J. E. McEnery, P. F. Michelson, W. Mitthumsiri, T. Mizuno, A. A. Moiseev, M. E. Monzani, A. Morselli, I. V. Moskalenko, S. Murgia, R. Nemmen, E. Nuss, T. Ohsugi, N. Omodei, E. Orlando, J. F. Ormes, D. Paneque, J. H. Panetta, J. S. Perkins, M. Pesce-Rollins, F. Piron, G. Pivato, T. A. Porter, S. Rainò, R. Rando, M. Razzano, S. Razzaque, A. Reimer, O. Reimer, T. Reposeur, S. Ritz, R. W. Romani, M. Sánchez-Conde, M. Schaal, A. Schulz, C. Sgrò, E. J. Siskind, G. Spandre, P. Spinelli, A. W. Strong, D. J. Suson, H. Takahashi, J. G. Thayer, J. B. Thayer, L. Tibaldo, M. Tinivella, D. F. Torres, G. Tosti, E. Troja, Y. Uchiyama, G. Vianello, M. Werner, B. L. Winer, K. S. Wood, M. Wood, G. Zaharijas, S. Zimmer, The Spectrum of Isotropic Diffuse Gamma-Ray Emission between 100 MeV and 820 GeV, *ApJ* 799 (2015) 86 (Jan. 2015). [arXiv:1410.3696](https://arxiv.org/abs/1410.3696), [doi:10.1088/0004-637X/799/1/86](https://doi.org/10.1088/0004-637X/799/1/86).
- [13] X. Wang, A. Loeb, Contribution of quasar-driven outflows to the extragalactic gamma-ray background, *Nature Physics* 12 (2016) 1116–1118 (Dec. 2016). [doi:10.1038/nphys3837](https://doi.org/10.1038/nphys3837).
- [14] A. Lamastra, N. Menci, F. Fiore, L. A. Antonelli, S. Colafrancesco, D. Guetta, A. Stamerra, Extragalactic gamma-ray background from AGN winds and star-forming galaxies in cosmological galaxy-formation models, *A&A* 607 (2017) A18 (Oct. 2017). [arXiv:1709.03497](https://arxiv.org/abs/1709.03497), [doi:10.1051/0004-6361/201731452](https://doi.org/10.1051/0004-6361/201731452).
- [15] R.-Y. Liu, K. Murase, S. Inoue, C. Ge, X.-Y. Wang, Can Winds Driven by Active Galactic Nuclei Account for the Extragalactic Gamma-Ray and Neutrino Backgrounds?, *ApJ* 858 (2018) 9 (May 2018). [arXiv:1712.10168](https://arxiv.org/abs/1712.10168), [doi:10.3847/1538-4357/aaba74](https://doi.org/10.3847/1538-4357/aaba74).
- [16] M. Krips, S. Martín, A. Eckart, R. Neri, S. García-Burillo, S. Matsushita, A. Peck, I. Stoklasová, G. Petitpas, A. Usero, F. Combes,

- E. Schinnerer, E. Humphreys, A. J. Baker, Submillimeter Array/Plateau de Bure Interferometer Multiple Line Observations of the Nearby Seyfert 2 Galaxy NGC 1068: Shock-related Gas Kinematics and Heating in the Central 100 pc?, *ApJ* 736 (2011) 37 (Jul. 2011). [arXiv:1105.6089](https://arxiv.org/abs/1105.6089), [doi:10.1088/0004-637X/736/1/37](https://doi.org/10.1088/0004-637X/736/1/37).
- [17] S. García-Burillo, F. Combes, A. Usero, S. Aalto, M. Krips, S. Viti, A. Alonso-Herrero, L. K. Hunt, E. Schinnerer, A. J. Baker, F. Boone, V. Casasola, L. Colina, F. Costagliola, A. Eckart, A. Fuente, C. Henkel, A. Labiano, S. Martín, I. Márquez, S. Muller, P. Planesas, C. Ramos Almeida, M. Spaans, L. J. Tacconi, P. P. van der Werf, Molecular line emission in NGC 1068 imaged with ALMA. I. An AGN-driven outflow in the dense molecular gas, *A&A* 567 (2014) A125 (Jul. 2014). [arXiv:1405.7706](https://arxiv.org/abs/1405.7706), [doi:10.1051/0004-6361/201423843](https://doi.org/10.1051/0004-6361/201423843).
- [18] J. F. Gallimore, S. A. Baum, C. P. O’Dea, A. Pedlar, The Subarcsecond Radio Structure in NGC 1068. I. Observations and Results, *ApJ* 458 (1996) 136 (Feb. 1996). [doi:10.1086/176798](https://doi.org/10.1086/176798).
- [19] C. G. Wynn-Williams, E. E. Becklin, N. Z. Scoville, The 3 kiloparsec radio disk and halo of NGC 1068, *ApJ* 297 (1985) 607–610 (Oct. 1985). [doi:10.1086/163557](https://doi.org/10.1086/163557).
- [20] J. F. Gallimore, D. J. Axon, C. P. O’Dea, S. A. Baum, A. Pedlar, A Survey of Kiloparsec-Scale Radio Outflows in Radio-Quiet Active Galactic Nuclei, *AJ* 132 (2006) 546–569 (Aug. 2006). [arXiv:astro-ph/0604219](https://arxiv.org/abs/astro-ph/0604219), [doi:10.1086/504593](https://doi.org/10.1086/504593).
- [21] A. Sajina, B. Partridge, T. Evans, S. Steff, N. Vechik, S. Myers, S. Dicker, P. Korngut, High-frequency Radio Spectral Energy Distributions and Polarization Fractions of Sources in an Atacama Cosmology Telescope Survey Field, *ApJ* 732 (2011) 45 (May 2011). [doi:10.1088/0004-637X/732/1/45](https://doi.org/10.1088/0004-637X/732/1/45).
- [22] S. F. Hönic, M. A. Prieto, T. Beckert, High-spatial resolution SED of NGC 1068 from near-IR to radio. Disentangling the thermal and non-thermal contributions, *A&A* 485 (2008) 33–39 (Jul. 2008). [arXiv:0804.0236](https://arxiv.org/abs/0804.0236), [doi:10.1051/0004-6361:200809606](https://doi.org/10.1051/0004-6361:200809606).

- [23] T. M. Yoast-Hull, J. S. Gallagher, III, E. G. Zweibel, J. E. Everett, Active Galactic Nuclei, Neutrinos, and Interacting Cosmic Rays in NGC 253 and NGC 1068, *ApJ* 780 (2014) 137 (Jan. 2014). [arXiv:1311.5586](#), [doi:10.1088/0004-637X/780/2/137](#).
- [24] B. Eichmann, J. Becker Tjus, The Radio-Gamma Correlation in Starburst Galaxies, *ApJ* 821 (2016) 87 (Apr. 2016). [arXiv:1510.03672](#), [doi:10.3847/0004-637X/821/2/87](#).
- [25] A. Lamastra, F. Fiore, D. Guetta, L. A. Antonelli, S. Colafrancesco, N. Menci, S. Puccetti, A. Stameria, L. Zappacosta, Galactic outflow driven by the active nucleus and the origin of the gamma-ray emission in NGC 1068, *A&A* 596 (2016) A68 (Dec. 2016). [arXiv:1609.09664](#), [doi:10.1051/0004-6361/201628667](#).
- [26] J.-P. Lenain, C. Ricci, M. Türler, D. Dorner, R. Walter, Seyfert 2 galaxies in the GeV band: jets and starburst, *A&A* 524 (2010) A72 (Dec. 2010). [arXiv:1008.5164](#), [doi:10.1051/0004-6361/201015644](#).
- [27] J. Nims, E. Quataert, C.-A. Faucher-Giguère, Observational signatures of galactic winds powered by active galactic nuclei, *MNRAS* 447 (2015) 3612–3622 (Mar. 2015). [arXiv:1408.5141](#), [doi:10.1093/mnras/stu2648](#).
- [28] C. Bustard, E. G. Zweibel, C. Cotter, Cosmic Ray Acceleration by a Versatile Family of Galactic Wind Termination Shocks, *ApJ* 835 (2017) 72 (Jan. 2017). [arXiv:1610.06565](#), [doi:10.3847/1538-4357/835/1/72](#).
- [29] G. E. Romero, A. L. Müller, M. Roth, Particle acceleration in the superwinds of starburst galaxies, *A&A* 616 (2018) A57 (Aug. 2018). [arXiv:1801.06483](#), [doi:10.1051/0004-6361/201832666](#).
- [30] A. R. Bell, The acceleration of cosmic rays in shock fronts. I, *MNRAS* 182 (1978) 147–156 (Jan. 1978). [doi:10.1093/mnras/182.2.147](#).
- [31] A. R. Bell, The acceleration of cosmic rays in shock fronts. II, *MNRAS* 182 (1978) 443–455 (Feb. 1978). [doi:10.1093/mnras/182.3.443](#).
- [32] R. D. Blandford, J. P. Ostriker, Particle acceleration by astrophysical shocks, *ApJL* 221 (1978) L29–L32 (Apr. 1978). [doi:10.1086/182658](#).

- [33] L. Drury, On particle acceleration in supernova remnants, *Space Sci. Rev.* 36 (1983) 57–60 (Sep. 1983). doi:10.1007/BF00171901.
- [34] T. Robishaw, E. Quataert, C. Heiles, Extragalactic Zeeman Detections in OH Megamasers, *ApJ* 680 (2008) 981–998 (Jun. 2008). arXiv:0803.1832, doi:10.1086/588031.
- [35] B. C. Lacki, T. A. Thompson, E. Quataert, The Physics of the Far-infrared-Radio Correlation. I. Calorimetry, Conspiracy, and Implications, *ApJ* 717 (2010) 1–28 (Jul. 2010). arXiv:0907.4161, doi:10.1088/0004-637X/717/1/1.
- [36] J. McBride, E. Quataert, C. Heiles, A. Bauermeister, The Role of Magnetic Fields in Starburst Galaxies as Revealed by OH Megamasers, *ApJ* 780 (2014) 182 (Jan. 2014). arXiv:1310.1957, doi:10.1088/0004-637X/780/2/182.
- [37] E. Schinnerer, A. Eckart, L. J. Tacconi, R. Genzel, D. Downes, Bars and Warps Traced by the Molecular Gas in the Seyfert 2 Galaxy NGC 1068, *ApJ* 533 (2000) 850–868 (Apr. 2000). arXiv:astro-ph/9911488, doi:10.1086/308702.
- [38] S. Y. Sazonov, J. P. Ostriker, R. A. Sunyaev, Quasars: the characteristic spectrum and the induced radiative heating, *MNRAS* 347 (2004) 144–156 (Jan. 2004). arXiv:astro-ph/0305233, doi:10.1111/j.1365-2966.2004.07184.x.
- [39] J. J. Bock, G. Neugebauer, K. Matthews, B. T. Soifer, E. E. Becklin, M. Ressler, K. Marsh, M. W. Werner, E. Egami, R. Blandford, High Spatial Resolution Imaging of NGC 1068 in the Mid-Infrared, *AJ* 120 (2000) 2904–2919 (Dec. 2000). arXiv:astro-ph/0009078, doi:10.1086/316871.
- [40] A. Alonso-Herrero, C. Ramos Almeida, R. Mason, A. Asensio Ramos, P. F. Roche, N. A. Levenson, M. Elitzur, C. Packham, J. M. Rodríguez Espinosa, S. Young, T. Díaz-Santos, A. M. Pérez-García, Torus and Active Galactic Nucleus Properties of Nearby Seyfert Galaxies: Results from Fitting Infrared Spectral Energy Distributions and Spectroscopy, *ApJ* 736 (2011) 82 (Aug. 2011). arXiv:1105.2368, doi:10.1088/0004-637X/736/2/82.

- [41] A. Marinucci, S. Bianchi, G. Matt, D. M. Alexander, M. Baloković, F. E. Bauer, W. N. Brandt, P. Gandhi, M. Guainazzi, F. A. Harrison, K. Iwasawa, M. Koss, K. K. Madsen, F. Nicastro, S. Puccetti, C. Ricci, D. Stern, D. J. Walton, NuSTAR catches the unveiling nucleus of NGC 1068, *MNRAS* 456 (2016) L94–L98 (Feb. 2016). [arXiv:1511.03503](#), [doi:10.1093/mnrasl/slv178](#).
- [42] E. Peretti, P. Blasi, F. Aharonian, G. Morlino, Cosmic ray transport and radiative processes in nuclei of starburst galaxies, *arXiv e-prints* (Dec. 2018). [arXiv:1812.01996](#).
- [43] L. Spinoglio, M. A. Malkan, H. A. Smith, E. González-Alfonso, J. Fischer, The Far-Infrared Emission Line and Continuum Spectrum of the Seyfert Galaxy NGC 1068, *ApJ* 623 (2005) 123–136 (Apr. 2005). [arXiv:astro-ph/0501024](#), [doi:10.1086/428495](#).
- [44] A. Domínguez, J. R. Primack, D. J. Rosario, F. Prada, R. C. Gilmore, S. M. Faber, D. C. Koo, R. S. Somerville, M. A. Pérez-Torres, P. Pérez-González, J.-S. Huang, M. Davis, P. Guhathakurta, P. Barmby, C. J. Conselice, M. Lozano, J. A. Newman, M. C. Cooper, Extragalactic background light inferred from AEGIS galaxy-SED-type fractions, *MNRAS* 410 (2011) 2556–2578 (Feb. 2011). [arXiv:1007.1459](#), [doi:10.1111/j.1365-2966.2010.17631.x](#).
- [45] V. Berezhinsky, O. Kalashev, High-energy electromagnetic cascades in extragalactic space: Physics and features, *PRD* 94 (2) (2016) 023007 (Jul. 2016). [arXiv:1603.03989](#), [doi:10.1103/PhysRevD.94.023007](#).
- [46] F. Acero, M. Ackermann, M. Ajello, A. Albert, W. B. Atwood, M. Axelsson, L. Baldini, J. Ballet, G. Barbiellini, D. Bastieri, A. Belfiore, R. Bellazzini, E. Bissaldi, R. D. Blandford, E. D. Bloom, J. R. Bogart, R. Bonino, E. Bottacini, J. Bregeon, R. J. Britto, P. Bruel, R. Buehler, T. H. Burnett, S. Buson, G. A. Caliandro, R. A. Cameron, R. Caputo, M. Caragiulo, P. A. Caraveo, J. M. Casandjian, E. Cavazzuti, E. Charles, R. C. G. Chaves, A. Chekhtman, C. C. Cheung, J. Chiang, G. Chiaro, S. Ciprini, R. Claus, J. Cohen-Tanugi, L. R. Cominsky, J. Conrad, S. Cutini, F. D’Ammando, A. de Angelis, M. DeKlotz, F. de Palma, R. Desiante, S. W. Digel, L. Di Venere, P. S. Drell, R. Dubois, D. Dumora, C. Favuzzi, S. J. Fegan, E. C. Ferrara, J. Finke,

A. Franckowiak, Y. Fukazawa, S. Funk, P. Fusco, F. Gargano, D. Gasparri, B. Giebels, N. Giglietto, P. Giommi, F. Giordano, M. Giroletti, T. Glanzman, G. Godfrey, I. A. Grenier, M.-H. Grondin, J. E. Grove, L. Guillemot, S. Guiriec, D. Hadasch, A. K. Harding, E. Hays, J. W. Hewitt, A. B. Hill, D. Horan, G. Iafrate, T. Jogler, G. Jóhannesson, R. P. Johnson, A. S. Johnson, T. J. Johnson, W. N. Johnson, T. Kamae, J. Kataoka, J. Katsuta, M. Kuss, G. La Mura, D. Landriu, S. Larsson, L. Latronico, M. Lemoine-Goumard, J. Li, L. Li, F. Longo, F. Loparco, B. Lott, M. N. Lovellette, P. Lubrano, G. M. Madejski, F. Massaro, M. Mayer, M. N. Mazziotta, J. E. McEnery, P. F. Michelson, N. Mirabal, T. Mizuno, A. A. Moiseev, M. Mongelli, M. E. Monzani, A. Morselli, I. V. Moskalenko, S. Murgia, E. Nuss, M. Ohno, T. Ohsugi, N. Omodei, M. Orienti, E. Orlando, J. F. Ormes, D. Paneque, J. H. Panetta, J. S. Perkins, M. Pesce-Rollins, F. Piron, G. Pivato, T. A. Porter, J. L. Racusin, R. Rando, M. Razzano, S. Razzaque, A. Reimer, O. Reimer, T. Reposeur, L. S. Rochester, R. W. Romani, D. Salvetti, M. Sánchez-Conde, P. M. Saz Parkinson, A. Schulz, E. J. Siskind, D. A. Smith, F. Spada, G. Spandre, P. Spinelli, T. E. Stephens, A. W. Strong, D. J. Suson, H. Takahashi, T. Takahashi, Y. Tanaka, J. G. Thayer, J. B. Thayer, D. J. Thompson, L. Tibaldo, O. Tibolla, D. F. Torres, E. Torresi, G. Tosti, E. Troja, B. Van Klaveren, G. Vianello, B. L. Winer, K. S. Wood, M. Wood, S. Zimmer, Fermi-LAT Collaboration, Fermi Large Area Telescope Third Source Catalog, *ApJS* 218 (2015) 23 (Jun. 2015). [arXiv:1501.02003](https://arxiv.org/abs/1501.02003), [doi:10.1088/0067-0049/218/2/23](https://doi.org/10.1088/0067-0049/218/2/23).

- [47] M. Ajello, W. B. Atwood, L. Baldini, J. Ballet, G. Barbiellini, D. Bastieri, R. Bellazzini, E. Bissaldi, R. D. Blandford, E. D. Bloom, R. Bonino, J. Bregeon, R. J. Britto, P. Bruel, R. Buehler, S. Buson, R. A. Cameron, R. Caputo, M. Caragiulo, P. A. Caraveo, E. Cavazzuti, C. Cecchi, E. Charles, A. Chekhtman, C. C. Cheung, G. Chiaro, S. Ciprini, J. M. Cohen, D. Costantin, F. Costanza, A. Cuoco, S. Cutini, F. D’Ammando, F. de Palma, R. Desiante, S. W. Digel, N. Di Lalla, M. Di Mauro, L. Di Venere, A. Domínguez, P. S. Drell, D. Dumora, C. Favuzzi, S. J. Fegan, E. C. Ferrara, P. Fortin, A. Franckowiak, Y. Fukazawa, S. Funk, P. Fusco, F. Gargano, D. Gasparri, N. Giglietto, P. Giommi, F. Giordano, M. Giroletti, T. Glanzman, D. Green, I. A. Grenier, M.-H. Grondin, J. E. Grove, L. Guillemot, S. Guiriec, A. K. Harding, E. Hays, J. W. Hewitt, D. Horan, G. Jóhannesson,

- S. Kensei, M. Kuss, G. La Mura, S. Larsson, L. Latronico, M. Lemoine-Goumard, J. Li, F. Longo, F. Loparco, B. Lott, P. Lubrano, J. D. Magill, S. Maldera, A. Manfreda, M. N. Mazziotta, J. E. McEnery, M. Meyer, P. F. Michelson, N. Mirabal, W. Mitthumsiri, T. Mizuno, A. A. Moiseev, M. E. Monzani, A. Morselli, I. V. Moskalenko, M. Negro, E. Nuss, T. Ohsugi, N. Omodei, M. Orienti, E. Orlando, M. Palatiello, V. S. Paliya, D. Paneque, J. S. Perkins, M. Persic, M. Pesce-Rollins, F. Piron, T. A. Porter, G. Principe, S. Rainò, R. Rando, M. Razzano, S. Razzaque, A. Reimer, O. Reimer, T. Reposeur, P. M. Saz Parkinson, C. Sgrò, D. Simone, E. J. Siskind, F. Spada, G. Spandre, P. Spinelli, L. Stawarz, D. J. Suson, M. Takahashi, D. Tak, J. G. Thayer, J. B. Thayer, D. J. Thompson, D. F. Torres, E. Torresi, E. Troja, G. Vianello, K. Wood, M. Wood, 3FHL: The Third Catalog of Hard Fermi-LAT Sources, *ApJS* 232 (2017) 18 (Oct. 2017). [arXiv:1702.00664](https://arxiv.org/abs/1702.00664), [doi:10.3847/1538-4365/aa8221](https://doi.org/10.3847/1538-4365/aa8221).
- [48] L. Maraschi, F. Tavecchio, The Jet-Disk Connection and Blazar Unification, *ApJ* 593 (2003) 667–675 (Aug. 2003). [arXiv:astro-ph/0205252](https://arxiv.org/abs/astro-ph/0205252), [doi:10.1086/342118](https://doi.org/10.1086/342118).
- [49] J. Knödlseeder, M. Mayer, C. Deil, J.-B. Cayrou, E. Owen, N. Kelley-Hoskins, C.-C. Lu, R. Buehler, F. Forest, T. Louge, H. Siejkowski, K. Kosack, L. Gerard, A. Schulz, P. Martin, D. Sanchez, S. Ohm, T. Hassan, S. Brau-Nogué, GammaLib and ctools. A software framework for the analysis of astronomical gamma-ray data, *A&A* 593 (2016) A1 (Aug. 2016). [arXiv:1606.00393](https://arxiv.org/abs/1606.00393), [doi:10.1051/0004-6361/201628822](https://doi.org/10.1051/0004-6361/201628822).
- [50] M. Landoni, P. Romano, S. Vercellone, J. Knödlseeder, A. Bianco, F. Tavecchio, A. Corina, A Cloud-based Architecture for the Cherenkov Telescope Array Observation Simulations: Optimization, Design, and Results, *ApJS* 240 (2019) 32 (Feb. 2019). [arXiv:1901.00410](https://arxiv.org/abs/1901.00410), [doi:10.3847/1538-4365/aafcb5](https://doi.org/10.3847/1538-4365/aafcb5).
- [51] W. Cash, Parameter estimation in astronomy through application of the likelihood ratio, *ApJ* 228 (1979) 939–947 (Mar. 1979). [doi:10.1086/156922](https://doi.org/10.1086/156922).
- [52] J. R. Mattox, D. L. Bertsch, J. Chiang, B. L. Dingus, S. W. Digel, J. A. Esposito, J. M. Fierro, R. C. Hartman, S. D. Hunter, G. Kanbach, D. A. Kniffen, Y. C. Lin, D. J. Macomb, H. A. Mayer-Hasselwander,

- P. F. Michelson, C. von Montigny, R. Mukherjee, P. L. Nolan, P. V. Ramanamurthy, E. Schneid, P. Sreekumar, D. J. Thompson, T. D. Willis, The Likelihood Analysis of EGRET Data, *ApJ* 461 (1996) 396 (Apr. 1996). doi:10.1086/177068.
- [53] I. Tamborra, S. Ando, K. Murase, Star-forming galaxies as the origin of diffuse high-energy backgrounds: gamma-ray and neutrino connections, and implications for starburst history, *JCAP* 9 (2014) 043 (Sep. 2014). arXiv:1404.1189, doi:10.1088/1475-7516/2014/09/043.
- [54] X. Wang, A. Loeb, Cumulative neutrino background from quasar-driven outflows, *JCAP* 12 (2016) 012 (Dec. 2016). arXiv:1607.06476, doi:10.1088/1475-7516/2016/12/012.
- [55] M. G. Aartsen, M. Ackermann, J. Adams, J. A. Aguilar, M. Ahlers, M. Ahrens, D. Altmann, T. Anderson, C. Argüelles, T. C. Arlen, et al., Searches for Extended and Point-like Neutrino Sources with Four Years of IceCube Data, *ApJ* 796 (2014) 109 (Dec. 2014). doi:10.1088/0004-637X/796/2/109.
- [56] M. G. Aartsen, K. Abraham, M. Ackermann, J. Adams, J. A. Aguilar, M. Ahlers, M. Ahrens, D. Altmann, T. Anderson, M. Archinger, et al., A Combined Maximum-likelihood Analysis of the High-energy Astrophysical Neutrino Flux Measured with IceCube, *ApJ* 809 (2015) 98 (Aug. 2015). arXiv:1507.03991, doi:10.1088/0004-637X/809/1/98.
- [57] U. Keshet, E. Waxman, A. Loeb, V. Springel, L. Hernquist, Gamma Rays from Intergalactic Shocks, *ApJ* 585 (2003) 128–150 (Mar. 2003). arXiv:astro-ph/0202318, doi:10.1086/345946.
- [58] T. A. Thompson, E. Quataert, E. Waxman, N. Murray, C. L. Martin, Magnetic Fields in Starburst Galaxies and the Origin of the FIR-Radio Correlation, *ApJ* 645 (2006) 186–198 (Jul. 2006). arXiv:astro-ph/0601626, doi:10.1086/504035.
- [59] V. Tatischeff, Cosmic-ray acceleration in supernova shocks, [ArXiv:0804.1004] (Apr. 2008). arXiv:0804.1004.
- [60] R. Wojaczyński, A. Niedźwiecki, The X-/ γ -Ray Correlation in NGC 4945 and the Nature of Its γ -Ray Source, *ApJ* 849 (2017) 97 (Nov. 2017). arXiv:1710.01847, doi:10.3847/1538-4357/aa8f9d.

- [61] X. Wang, B. D. Fields, Are starburst galaxies proton calorimeters?, *MNRAS* 474 (2018) 4073–4088 (Mar. 2018). [arXiv:1612.07290](#), [doi:10.1093/mnras/stx2917](#).
- [62] L. K. Zschaechner, F. Walter, A. Bolatto, E. P. Farina, J. M. D. Kruijssen, A. Leroy, D. S. Meier, J. Ott, S. Veilleux, The Molecular Wind in the Nearest Seyfert Galaxy Circinus Revealed by ALMA, *ApJ* 832 (2016) 142 (Dec. 2016). [arXiv:1609.06316](#), [doi:10.3847/0004-637X/832/2/142](#).
- [63] C. Henkel, S. Muehle, G. Bendo, G. I. G. Jozsa, Y. Gong, S. Viti, S. Aalto, F. Combes, S. Garcia-Burillo, L. K. Hunt, J. Mangum, S. Martin, S. Muller, J. Ott, P. van der Werf, A. A. Malawi, H. Ismail, F. Alkhuja, H. M. Asiri, R. Aladro, F. Alves, Y. Ao, W. A. Baan, F. Costagliola, G. Fuller, J. Greene, C. M. V. Impellizzeri, F. Kamali, R. S. Klessen, R. Mauersberger, X. D. Tang, K. Tristram, M. Wang, J. S. Zhang, Molecular line emission in NGC 4945, imaged with ALMA, *ArXiv e-prints* (Feb. 2018). [arXiv:1802.09852](#).
- [64] M. Elmouttie, R. F. Haynes, K. L. Jones, E. M. Sadler, M. Ehle, Radio continuum evidence for nuclear outflow in the Circinus galaxy, *MNRAS* 297 (1998) 1202–1218 (Jul. 1998). [doi:10.1046/j.1365-8711.1998.01592.x](#).
- [65] E. Lenc, S. J. Tingay, The Sub-Parsec Scale Radio Properties of Southern Starburst Galaxies. II. Supernova Remnants, the Supernova Rate, and the Ionised Medium in the NGC 4945 Starburst, *AJ* 137 (2009) 537–553 (Jan. 2009). [arXiv:0811.0057](#), [doi:10.1088/0004-6256/137/1/537](#).
- [66] R. Wojaczyński, A. Niedźwiecki, F.-G. Xie, M. Szanecki, Gamma-ray activity of Seyfert galaxies and constraints on hot accretion flows, *A&A* 584 (2015) A20 (Dec. 2015). [arXiv:1505.07608](#), [doi:10.1051/0004-6361/201526621](#).
- [67] VERITAS Collaboration, V. A. Acciari, E. Aliu, T. Arlen, T. Aune, M. Bautista, M. Beilicke, W. Benbow, D. Boltuch, S. M. Bradbury, J. H. Buckley, V. Bugaev, K. Byrum, A. Cannon, O. Celik, A. Cesarini, Y. C. Chow, L. Ciupik, P. Cogan, P. Colin, W. Cui, R. Dickherber, C. Duke,

S. J. Fegan, J. P. Finley, G. Finnegan, P. Fortin, L. Fortson, A. Furniss, N. Galante, D. Gall, K. Gibbs, G. H. Gillanders, S. Godambe, J. Grube, R. Guenette, G. Gyuk, D. Hanna, J. Holder, D. Horan, C. M. Hui, T. B. Humensky, A. Imran, P. Kaaret, N. Karlsson, M. Kertzman, D. Kieda, J. Kildea, A. Konopelko, H. Krawczynski, F. Krennrich, M. J. Lang, S. Lebohec, G. Maier, S. McArthur, A. McCann, M. McCutcheon, J. Millis, P. Moriarty, R. Mukherjee, T. Nagai, R. A. Ong, A. N. Otte, D. Pandel, J. S. Perkins, F. Pizlo, M. Pohl, J. Quinn, K. Ragan, L. C. Reyes, P. T. Reynolds, E. Roache, H. J. Rose, M. Schroedter, G. H. Sembroski, A. W. Smith, D. Steele, S. P. Swordy, M. Theiling, S. Thibadeau, A. Varlotta, V. V. Vassiliev, S. Vincent, R. G. Wagner, S. P. Wakely, J. E. Ward, T. C. Weekes, A. Weinstein, T. Weisgarber, D. A. Williams, S. Wissel, M. Wood, B. Zitzer, A connection between star formation activity and cosmic rays in the starburst galaxy M82, *Nature* 462 (2009) 770–772 (Dec. 2009). [arXiv:0911.0873](https://arxiv.org/abs/0911.0873), [doi:10.1038/nature08557](https://doi.org/10.1038/nature08557).

- [68] A. Abramowski, F. Acero, F. Aharonian, A. G. Akhperjanian, G. Anton, A. Balzer, A. Barnacka, Y. Becherini, J. Becker, K. Bernlöhner, E. Birsin, J. Biteau, A. Bochow, C. Boisson, J. Bolmont, P. Bordas, J. Brucker, F. Brun, P. Brun, T. Bulik, I. Büsching, S. Carrigan, S. Casanova, M. Cerruti, P. M. Chadwick, A. Charbonnier, R. C. G. Chaves, A. Cheesebrough, G. Cologna, J. Conrad, C. Couturier, M. Dalton, M. K. Daniel, I. D. Davids, B. Degrange, C. Deil, H. J. Dickinson, A. Djannati-Ataï, W. Domainko, L. O. Drury, G. Dubus, K. Dutton, J. Dyks, M. Dyrda, K. Egberts, P. Eger, P. Espigat, L. Fallon, S. Fegan, F. Feinstein, M. V. Fernandes, A. Fiasson, G. Fontaine, A. Förster, M. Füßling, M. Gajdus, Y. A. Gallant, T. Garrigoux, H. Gast, L. Gérard, B. Giebels, J. F. Glicenstein, B. Glück, D. Göring, M.-H. Grondin, S. Häffner, J. D. Hague, J. Hahn, D. Hampf, J. Harris, M. Hauser, S. Heinz, G. Heinzlmann, G. Henri, G. Hermann, A. Hillert, J. A. Hinton, W. Hofmann, P. Hofverberg, M. Holler, D. Horns, A. Jacholkowska, C. Jahn, M. Jamroz, I. Jung, M. A. Kastendieck, K. Katarzyński, U. Katz, S. Kaufmann, B. Khélifi, D. Klochov, W. Kluźniak, T. Kneiske, N. Komin, K. Kosack, R. Kossakowski, F. Krayzel, H. Laffon, G. Lamanna, J.-P. Lenain, D. Lennarz, T. Lohse, A. Lopatin, C.-C. Lu, V. Marandon, A. Marcowith, J. Masbou, G. Maurin, N. Maxted, M. Mayer, T. J. L. McComb, M. C. Medina, J. Méhault, R. Moderski, M. Mohamed, E. Moulin, C. L. Naumann, M. Naumann-

Godo, M. de Naurois, D. Nedbal, D. Nekrassov, N. Nguyen, B. Nicholas, J. Niemiec, S. J. Nolan, S. Ohm, E. de Oña Wilhelmi, B. Opitz, M. Ostrowski, I. Oya, M. Panter, M. Paz Arribas, N. W. Pekeur, G. Pelletier, J. Perez, P.-O. Petrucci, B. Peyaud, S. Pita, G. Pühlhofer, M. Punch, A. Quirrenbach, M. Raue, A. Reimer, O. Reimer, M. Renaud, R. de los Reyes, F. Rieger, J. Ripken, L. Rob, S. Rosier-Lees, G. Rowell, B. Rudak, C. B. Rulten, V. Sahakian, D. A. Sanchez, A. Santangelo, R. Schlickeiser, A. Schulz, U. Schwanke, S. Schwarzburg, S. Schwemmer, F. Sheidaei, J. L. Skilton, H. Sol, G. Spengler, L. Stawarz, R. Steenkamp, C. Stegmann, F. Stinzinger, K. Stycz, I. Sushch, A. Szostek, J.-P. Taverne, R. Terrier, M. Tluczykont, K. Valerius, C. van Eldik, G. Vasileiadis, C. Venter, A. Viana, P. Vincent, H. J. Völk, F. Volpe, S. Vorobiov, M. Vorster, S. J. Wagner, M. Ward, R. White, A. Wierzcholska, M. Zacharias, A. Zajczyk, A. A. Zdziarski, A. Zech, H.-S. Zechlin, H. E. S. S. Collaboration, Spectral Analysis and Interpretation of the γ -Ray Emission from the Starburst Galaxy NGC 253, *ApJ* 757 (2012) 158 (Oct. 2012). [arXiv:1205.5485](https://arxiv.org/abs/1205.5485), [doi:10.1088/0004-637X/757/2/158](https://doi.org/10.1088/0004-637X/757/2/158).

- [69] H. E. S. S. Collaboration, H. Abdalla, F. Aharonian, F. Ait Benkhali, E. O. Angüner, M. Arakawa, C. Arcaro, C. Armand, M. Arrieta, M. Backes, et al., The starburst galaxy NGC 253 revisited by H.E.S.S. and Fermi-LAT, *ArXiv e-prints* (Jun. 2018). [arXiv:1806.03866](https://arxiv.org/abs/1806.03866).
- [70] J. Albert, E. Aliu, H. Anderhub, P. Antoranz, A. Armada, C. Baixeras, J. A. Barrio, H. Bartko, D. Bastieri, J. Becker, W. Bednarek, K. Berger, C. Bigongiari, A. Biland, R. K. Bock, P. Bordas, V. Bosch-Ramon, T. Bretz, I. Britvitch, M. Camara, E. Carmona, A. Chilingarian, S. Ciprini, J. A. Coarasa, S. Commichau, J. L. Contreras, J. Cortina, V. Curtef, V. Danielyan, F. Dazzi, A. De Angelis, R. de los Reyes, B. De Lotto, E. Domingo-Santamaría, D. Dorner, M. Doro, M. Errando, M. Fagiolini, D. Ferenc, E. Fernández, R. Firpo, J. Flix, M. V. Fonseca, L. Font, M. Fuchs, N. Galante, M. Garczarczyk, M. Gaug, M. Giller, F. Goebel, D. Hakobyan, M. Hayashida, T. Hengstebeck, D. Höhne, J. Hose, C. C. Hsu, P. Jacon, T. Jogler, O. Kalekin, R. Kosyra, D. Kranich, R. Kritzer, A. Laille, P. Liebing, E. Lindfors, S. Lombardi, F. Longo, J. López, M. López, E. Lorenz, P. Majumdar, G. Maneva, K. Mannheim, O. Mansutti, M. Mariotti, M. Martínez, D. Mazin, C. Merck, M. Meucci, M. Meyer, J. M. Miranda, R. Mirzoyan, S. Mi-

- zobuchi, A. Moralejo, K. Nilsson, J. Ninkovic, E. Oña-Wilhelmi, N. Otte, I. Oya, D. Paneque, R. Paoletti, J. M. Paredes, M. Pasanen, D. Pascoli, F. Pauss, R. Pegna, M. Persic, L. Peruzzo, A. Piccioli, M. Poller, N. Puchades, E. Prandini, A. Raymers, W. Rhode, M. Ribó, J. Rico, M. Rissi, A. Robert, S. Rügamer, A. Saggion, A. Sánchez, P. Sartori, V. Scalzotto, V. Scapin, R. Schmitt, T. Schweizer, M. Shayduk, K. Shinozaki, S. N. Shore, N. Sidro, A. Sillanpää, D. Sobczynska, A. Stamerra, L. S. Stark, L. Takalo, P. Temnikov, D. Tescaro, M. Teshima, N. Tonello, D. F. Torres, N. Turini, H. Vankov, V. Vitale, R. M. Wagner, T. Wibig, W. Wittek, R. Zanin, J. Zapatero, First Bounds on the Very High Energy γ -Ray Emission from Arp 220, *ApJ* 658 (2007) 245–248 (Mar. 2007). [arXiv:astro-ph/0611786](#), [doi:10.1086/511173](#).
- [71] H. Fleischhack, for the VERITAS collaboration, Upper limits on the VHE γ -ray flux from the ULIRG Arp 220 and other galaxies with VERITAS, ArXiv e-prints (Aug. 2015). [arXiv:1508.05807](#).
- [72] Q.-W. Tang, X.-Y. Wang, P.-H. T. Tam, Discovery of GeV Emission from the Direction of the Luminous Infrared Galaxy NGC 2146, *ApJ* 794 (2014) 26 (Oct. 2014). [arXiv:1407.3391](#), [doi:10.1088/0004-637X/794/1/26](#).
- [73] F.-K. Peng, X.-Y. Wang, R.-Y. Liu, Q.-W. Tang, J.-F. Wang, First Detection of GeV Emission from an Ultraluminous Infrared Galaxy: Arp 220 as Seen with the Fermi Large Area Telescope, *ApJL* 821 (2016) L20 (Apr. 2016). [arXiv:1603.06355](#), [doi:10.3847/2041-8205/821/2/L20](#).